THE JOURNAL OF PHYSICAL CHEMISTRY B

Article

pubs.acs.org/JPCB

In Situ Unfolded Lysozyme Induces the Lipid Lateral Redistribution of a Mixed Lipid Model Membrane

Jun-Jie Luo, Fu-Gen Wu, Shan-Shan Qin, and Zhi-Wu Yu*

Key Laboratory of Bioorganic Phosphorous Chemistry and Chemical Biology (Ministry of Education), Department of Chemistry, Tsinghua University, Beijing 100084, People's Republic of China

ABSTRACT: Redistribution of charged lipids induced by polyelectrolytes is an intriguing phenomenon. Proteins, due to their nature as polyelectrolytes, should also have this capacity. But their highly ordered structures may bring about more complex mechanisms. We studied the interaction between positively charged lysozyme and liposomes consisting of neutral dipalmitoylphosphatidylcholine (DPPC) and negatively charged dioleoylphosphatidylglycerol (DOPG). Interestingly, the enrichment of DOPG cannot be induced by the native and ex situ unfolded (unfolded in the absence of liposomes) lysozyme, but requires that lysozyme undergo an in situ unfolding process (unfolding in the presence of liposomes). These observations suggest that, for proteins, the capacity to induce lipid redistribution relies on not only the net charges but also the spatial distribution of the charges. During the in situ unfolding process, lysozyme reorganizes its structure into a specially unfolded structure that is rich in flat β-sheets and more "rigid" in the presence of lipid membrane. This special spatial structure changes the charge distribution and is advantageous to the protein−membrane electrostatic interaction and thus can induce lipid redistribution.

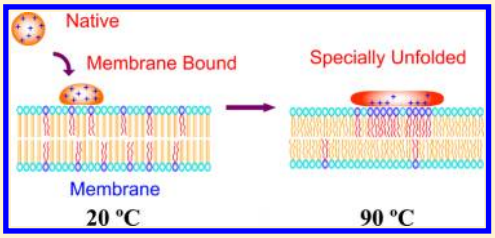

1. INTRODUCTION

Protein−membrane interactions exist widely in the biological and pathological activities of organisms.[1] These interactions pose impacts on both proteins and membranes, resulting in protein structural changes,[2−5] aggregation,[6−10] protein redistribution in bilayers,[11] membrane fusion,[12] pore or tubule formation,[13−15] vesicle budding,[16] and lipid flip-flop.[17] The fundamental underlying the membrane structural changes induced by protein binding is the modulation of lipid phase behaviors. In this regard, it has been found that protein binding can reduce the lipid lateral mobility[18,19] and influence the lipid packing order.[20]

Two interesting phenomena, the protein-induced lipid phase separation (or lipid "demixing") and protein structural changes upon membrane binding, have drawn the most attention in recent years. For the former, proteins, or peptides in most cases, due to their nature as polyelectrolytes, were demonstrated to be able to induce lipid phase separation.[21−28] Such protein-induced lipid phase separation is in fact the directionally lateral redistribution process of the lipid molecules within the membrane planes. In a study on a model membrane containing a charged species, theoretical calculation revealed that there was a significant increase in the charge density in the protein-bound membrane domains.[29] By using ^{31}P nuclear magnetic resonance (NMR) spectroscopy and fluorescence resonance energy transfer (FRET), lipid phase separation can be detected by investigating the structural properties of the lipid organizations.[30−32] Since a phase-separated membrane exhibits different main transition temperature (T_m) from that of a homogeneously mixed membrane, this enables the identification of lipid phase separation by differential scanning calorimetry (DSC).[33] On the other hand, many proteins were demonstrated to form β-sheet aggregated structures[34] or even amyloid fibers[8,35,36] upon membrane binding. This is particularly the case when the binding forms a densely packed protein layer on the membrane surface, leading to the deactivation of membrane-bound enzymes.[37] There has also been reports that the binding of β-lactoglobulin to dimyristoylphosphatidylglycerol (DMPG) membranes accompanies a β-sheet → α-helix structural transition.[38,39]

In most cases, the protein−membrane binding is initiated through the electrostatic interaction between the positively charged residues of proteins and the negatively charged lipid molecules, such as phosphatidylglycerol (PG)/phosphatidylserine (PS).[30,40,41] Besides, hydrophobic interaction is also involved in the interaction between proteins/peptides and lipids.[41−43] Among the positively charged proteins, lysozyme is a small (14.3 kDa, 129 amino acids) but highly positively charged (pI = ∼11.0, +7−8 at neutral pH) protein, with well-characterized structures.[44,45] Recently, the protein was found to be able to induce aggregation of cells and fusion of negatively charged vesicles.[46] Therefore, it becomes a very suitable model protein in studies of protein−membrane interactions, including protein-induced lipid phase separation. Moreover, proteins are different from common polyelectrolytes, because they have highly ordered secondary and tertiary structures. Their structures and structural changes during unfolding/refolding may exert a unique influence on the lipid phase behavior. This has been the focus of the present study.

Received: May 4, 2012
Revised: September 12, 2012
Published: September 26, 2012

In this work, we have studied the interactions between lysozyme and liposomes composed of a neutral phospholipid, 1,2-dipalmitoyl-*sn*-glycero-3-phosphocholine (DPPC), and the negatively charged 1,2-dioleoyl-*sn*-glycero-3-[phospho-*rac*-(1′-glycerol)] (DOPG), using DSC, circular dichroism (CD) spectroscopy, freeze-fracture electron microscopy (FFEM), and dynamic light scattering (DLS). The reason to select DPPC and DOPG in this work is the big difference in their main phase transition temperatures (T_m), 41[47,48] and −18 °C,[49] respectively. This makes it easier to detect the lipid phase behavior by DSC than in the case of two unsaturated lipids. Comparative experiments on the mixed lipids in the (1) absence of protein, (2) presence of native lysozyme, (3) presence of in situ unfolded lysozyme (thermally unfolded in the presence of liposomes), and (4) presence of ex situ unfolded lysozyme (thermally unfolded elsewhere and then mixed with liposomes at different temperatures) were carried out. It was found that only the in situ unfolded lysozyme could effectively induce lipid lateral redistribution. A mechanism focused on the protein spatial structures that were involved in the electrostatic interaction was built to describe this process.

2. EXPERIMENTAL SECTION

2.1. Sample Preparation. DPPC and DOPG were purchased from Avanti Polar Lipids (Birmingham, AL) and used without further purification. Lysozyme was purchased from Amresco (Solon, OH). Double deionized water with a resistivity of 18.2 MΩ·cm was used to prepare liposome and protein solutions. DPPC and DOPG lipids (4:1 molar ratio) were first dissolved in chloroform separately, and then mixed by vigorous vortexing to obtain a homogeneous solution. Subsequently, chloroform was evaporated under room temperature and the residual chloroform was removed under vacuum for 48 h. The dry lipid mixture was resuspended and rehydrated in 20 mM sodium phosphate buffer (pH 7.4) at 60 °C to form multilamellar vesicles with a total lipid concentration of 4 mg/mL. The vesicles were extruded through a polycarbonate membrane (100 nm diameter in pore size) 21 times at 60 °C to form large unilamellar vesicles (LUVs), using an Avanti miniextruder (Avanti Polar Lipids). The solution of LUVs was then cooled to ambient temperature in a water bath, at a cooling rate of 1 deg/min. Lysozyme was dissolved in the same sodium phosphate buffer (20 mM, pH 7.4) to reach a protein concentration of 2 mg/mL. To prepare the mixed lysozyme−liposome sample, equal volumes of lysozyme and liposome solutions were mixed to reach the protein to liposome ratio of 1:2 (1 and 2 mg/mL for each). The samples were equilibrated at ambient temperature for more than 30 min before measurements.

2.2. DLS. The extruded DPPC/DOPG liposome solutions were analyzed by DLS measurements to examine the size distribution. All the samples were examined at 25 °C with use of a Zetasizer 3000HS particle size analysis system (Malvern Instruments Ltd., Malvern, UK) at a scattering angle of 90°. The LUV solution at a total lipid concentration of 4 mg/mL was measured. Results were based on an average of 10 measurements.

2.3. FFEM. The morphologies of the liposome sample (2 mg/mL) and the mixed lysozyme−liposome sample (1 mg/mL protein and 2 mg/mL liposome) were characterized by FFEM technique.[50,51] A small drop of the solution or suspension equilibrated at 25 °C was sandwiched between two gold plates and manually plunged into liquid nitrogen. The standard freeze-fracture procedure was conducted in a Balzers BAF 400D freeze-fracture apparatus (BALZERS Ltd., LIE). Fractured surfaces were immediately shadowed at an angle of 45° with platinum/carbon. The platinum replica was then stabilized by deposition of pure carbon at an angle of 90°. Organic materials on the replicas were removed by washing in a methanol−chloroform (1/3, v/v) solution. Images of replicas were then examined and recorded on a JEOL 2010 transmission electron microscope (JEOL Ltd., Tokyo, Japan).

2.4. MicroDSC. All the calorimetric data were obtained on a CSC Model 6300 Nano III differential scanning calorimeter (Calorimetry Sciences Corp., Lindon, UT) with a capillary cell volume of 0.3 mL.[52,53] The heating and cooling scans were performed at a constant scan rate of 1 deg/min. Parallel measurements were conducted and the results agree very well. The error level was found to be very low (<2 μW) and its influences on the onset and peak temperatures are negligible.

2.5. CD. CD spectra were measured with a Chirascan CD spectrometer (Applied Photophysics Ltd., Leatherhead, UK).[53] Sample temperature was controlled by using a circulating water bath connected to a water-jacketed sample chamber. For measurements in the near-UV region (250−360 nm), a quartz cell with a path length of 0.5 cm was used, while for measurements in the far-UV region (180−260 nm), the cell path length was 0.1 cm. In near-UV measurements, the spectra of the phosphate buffer and the liposome solution (2 mg/mL) were used as the backgrounds for the spectra of the lysozyme sample (1 mg/mL) and mixed lysozyme−liposome sample (1 mg/mL lysozyme and 2 mg/mL liposome), respectively. In far-UV measurements, the concentrations of lysozyme and liposome were 0.25 and 0.5 mg/mL, respectively, in the lysozyme, liposome, and mixed lysozyme−liposome samples (where applicable). All the spectra of samples were further analyzed after subtracting those of backgrounds. The percentages of the secondary structures in lysozyme were obtained by fitting the far-UV CD spectra, using the CONTIN/LL method in the CDPro software package.[54,55]

3. RESULTS AND DISCUSSION

3.1. Lysozyme Induces the Flocculation of Liposomes. The size distribution and morphology of LUVs prepared by extrusion were examined by DLS and FFEM. As shown in Figure 1, the scattering intensity of the extruded LUVs shows a maximum at ∼100 nm, and this diameter slightly decreases after a heating−cooling scan. The FFEM image illustrated in the inset of Figure 1 shows the typical morphology of the liposomes.

The appearances of the solutions of liposome, lysozyme, and their mixture were examined. Their photographs taken during the sample preparation as described in section 2.1 are shown in Figure 2. When the translucent and light blue liposome solution (Figure 2A) was mixed with the transparent and colorless lysozyme solution (Figure 2B), white flocculent substances form immediately in the solution (Figure 2C). After standing or centrifugation, the floccules precipitate, leaving the transparent and colorless supernatant on the top of the vial (Figure 2D). The coagulation between liposomes and lysozyme is attributed to the electrostatic binding between the positively charged lysozyme and the negatively charged DOPG in the liposomes.

The microscopic morphology of the mixed lysozyme−liposome suspension (Figure 2C) was examined by FFEM technique. As shown in the overall image of the lysozyme−liposome mixture (Figure 2E), liposomes aggregate abundantly,

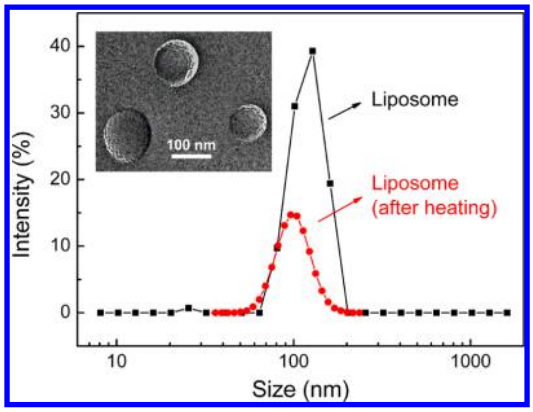

Figure 1. Size distributions of the DPPC/DOPG (4:1) liposomes detected by DLS. The black squares and the red circles depict the diameters of the extruded liposomes before and after a heating–cooling scan, respectively. The inset is an FFEM image of the extruded liposomes.

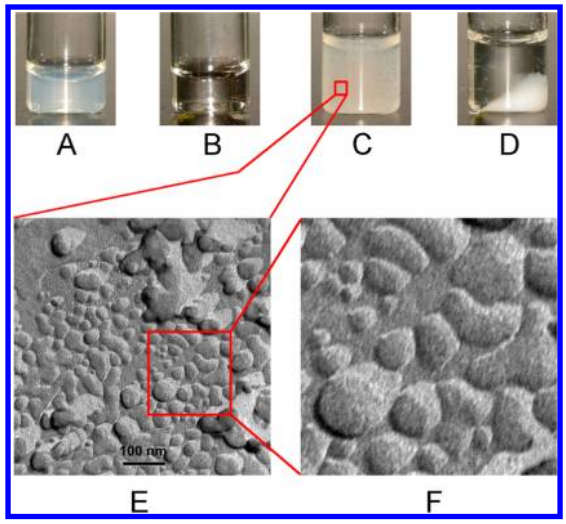

Figure 2. Photographs of (A) the liposomes, (B) the lysozyme, (C) the mixed lysozyme–liposome sample, and (D) the mixed sample after centrifugation. FFEM images (E and F) of the mixed lysozyme–liposome suspension.

forming random clusters. An enlarged picture of the clusters (Figure 2F) indicates the close contacts and adhesion between the liposomes. Some liposomes even deform to maximize their contact with each other. It is reasoned that lysozyme, with multisites for electrostatic binding, might have worked as bridges for the contact and adhesion between the charged liposomes.

3.2. Lysozyme Induces Lipid Phase Separation. The complete DSC curves in a heating–cooling–reheating cycle of the mixed lysozyme–liposome sample (the sample in Figure 2C) are shown in Figure 3A. The endothermic events of the sample in the first heating scan can be divided into two parts. The one in the temperature range below 40 °C corresponds to the lipid phase transition; the other above 60 °C belongs to the denaturation of lysozyme. To understand the influence of lysozyme on the lipid phase behaviors, the thermal property of the liposomes in the absence of the protein (the sample in Figure 2A) was examined as a control. As shown in Figure 3B (a, the black lines), in the first heating scan (the dash line), a sluggish endothermic profile ranging from 25 to 40 °C is seen, which is assigned as the lipid phase transition from lamellar gel (L_β) to lamellar liquid crystal phase (L_α). Two peaks with maxima at 34.0 and 31.1 °C overlap, indicating the coexistence of two types of mixed DPPC/DOPG microdomains with different lipid compositions. Because the T_m values of pure DPPC and DOPG are 41 and −18 °C, respectively, the peak with the higher temperature reflects a relatively higher composition of DPPC in the DPPC/DOPG microdomain. The reheating scan (the solid line) gives an almost identical endothermic profile as the first heating scan. But, for the mixed lysozyme–liposome sample (Figure 3A), the DSC heating–cooling–reheating scan shows a different feature. The low-temperature sections (20–50 °C) of the DSC heating scans in Figure 3A were also added into Figure 3B (b, the red lines) for the convenience of comparison. Compared to that of the free liposomes, the phase transition peak of the lysozyme-bound liposomes in the first heating scan is a little sharper and narrower (28–38 °C). But the shape of the phase transition peak is basically not affected by protein binding, showing overlapped peaks with a maximum at 33.0 °C and a shoulder at 29.8 °C.

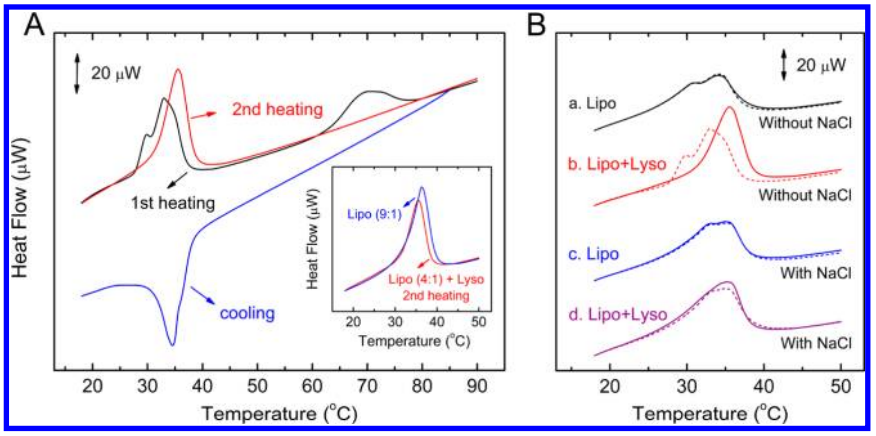

Figure 3. (A) DSC results of the mixed lysozyme–liposome sample in the heating–cooling–reheating scans. The inset is comparative DSC results of liposomes with different DPPC/DOPG ratios: the red line is the reheating scan of the mixed lysozyme and 4:1 DPPC/DOPG liposomes; the blue line is the heating scan of 9:1 DPPC/DOPG liposomes. (B) DSC results of the lipid phase transitions in the first (the dash lines) and second (the solid lines) heating scans.

dx.doi.org/10.1021/jp304339t | J. Phys. Chem. B 2012, 116, 12381–12388

More interestingly, in the reheating scan, a single endothermic peak at a higher temperature (35.6 °C) can be seen. This corresponds to the lipid phase transition in the DPPC-rich microdomains with a higher DPPC content, resulting from the enrichment of DOPG in the other class of microdomains whose phase transition temperature may have moved below the examined temperature range. Furthermore, the flip of the DOPG from the inner to the outer leaflet should also be involved in this process.[33] This is because the single sharp peak with a higher peak temperature must represent a uniform distribution of DOPG in both leaflets, which can only be achieved through the enrichment of DOPG in the outer leaflet accompanied by the transbilayer movement of DOPG from the inner to the outer leaflet. To verify this explanation, DSC measurement of a liposome sample with a DPPC/DOPG ratio of 9:1 was conducted and the result is shown in the inset of Figure 3A, together with the second heating of the lysozyme-bound liposomes (DPPC:DOPG = 4:1) for comparison. It can be seen that they exhibit nearly the same onset temperature. This strongly suggests that the DPPC-rich microdomains formed in the lysozyme-bound liposomes (DPPC:DOPG = 4:1) have a DPPC/DOPG ratio of 9:1. In addition, in the cooling scan (Figure 3A), the exothermic peak of lipid $L_\alpha \rightarrow L_\beta$ transition has lost the doublet feature.

The protein–membrane binding also exerts influence on protein structures. Shown in Figure 4 (curve b) is the

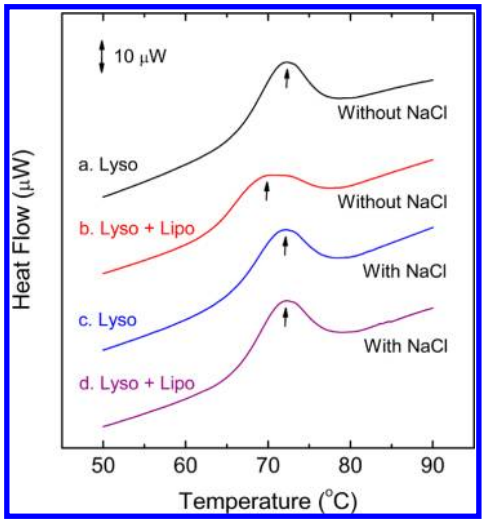

Figure 4. DSC results of lysozyme denaturation in the first heating scans.

denaturation peak of the liposome-bound lysozyme in the first heating scans, which is flatter than that of the free lysozyme (Figure 4, curve a), and the peak position shifts to a lower temperature for ~3 °C. This is consistent with the previous study on HSA and IgG upon membrane binding.[56] It indicates the reduction of thermal stability of lysozyme after binding to liposomes. Combining this phenomenon and that of the influence of proteins on the lipid phase behavior, we believe that there should be some intrinsic relationship between the enrichment of DOPG and the binding of lysozyme.

3.3. NaCl Screens the Electrostatic Binding between Lysozyme and Liposomes. To further investigate the electrostatic interactions between the enrichment of DOPG in liposomes and the binding of lysozyme, we examined the salt effect by adding 0.15 M NaCl to the phosphate buffer. With NaCl in the solutions, the appearances of the liposome and lysozyme solutions displayed no difference from those without NaCl to the naked eyes. But when they were mixed, the solution remained transparent and no precipitates were observed.

Thermal behaviors of the samples were examined. As shown in Figure 3B (c, the blue lines), in both the first and second heating scans of the liposome sample with NaCl, the $L_\beta \rightarrow L_\alpha$ phase transitions show overlapped peaks with two maxima at 33.1 and 35.1 °C. Compared to the sample without NaCl, the peak temperatures shift slightly to higher temperature, which is consistent with the previous study,[57] but the temperature range of the phase transition remains unchanged. As shown in Figure 3B (d, the purple lines), in the presence of NaCl, the mixed lysozyme–liposome sample produced similar overlapped endothermic peaks in the first heating scan as the free liposomes (Figure 3B, c), showing that they have similar phase behaviors. Then in the reheating scan, the lipid phase transition peak of the mixed lysozyme–liposome sample does not exhibit notable changes on the phase transition temperature as displayed in curve b, and only a little bit of an increase in the peak area is seen. In the presence of NaCl, the electrostatic repulsions between the negatively charged DOPG molecules would be screened owing to the higher ionic strength, which was supposed to allow the close contacts of DOPG molecules.[58] However, the observation demonstrates that the enrichment of DOPG cannot take place in the presence of NaCl.

As for the protein, the denaturation peaks of the free lysozyme without (Figure 4, curve a) or with NaCl (Figure 4, curve c) resemble each other, showing a single peak at ~72 °C. In the presence of NaCl, after the addition of liposomes, the denaturation peak of lysozyme (Figure 4, curve d) does not display any change. This is markedly different from what we observed for the liposome-bound lysozyme in the absence of NaCl (Figure 4, curve b). With NaCl in the solution, the electrostatic attractions between lysozyme and DOPG are screened, and thus the thermal behaviors of liposomes and lysozyme are independent. Therefore, the ionic strength effect observed in these experiments strongly suggests that the enrichment of DOPG is an electrostatically driven process: positively charged lysozyme induces the enrichment of negatively charged DOPG. This is equivalent to the formation of DPPC-rich microdomains.

3.4. Structural Changes of the Free and Liposome-Bound Lysozyme. The protein structural changes upon membrane binding can provide important clues for the mechanism of protein-induced lipid redistribution. The secondary structural changes of the free (ex situ) and the liposome-bound (in situ) lysozyme in heating–cooling–reheating scans, obtained by far-UV CD, are presented in parts A and B of Figure 5, respectively. We can see a remarkable increase in β-sheets and a decrease in α-helices, both by ~10%, and an increase in random coils, by ~5% in lysozyme after binding to liposomes. In the heating process of the liposome-bound lysozyme (Figure 5B), the fluctuation of β-sheet and α-helix structures between 25 and 35 °C corresponds to the stage of lipid phase transition. It is not a coincidence, but may reflect the rearrangement of protein structures induced by the lipid $L_\beta \rightarrow L_\alpha$ transition. Then, for both the free and the liposome-bound lysozyme, the abrupt changes of secondary structures start at 70 °C, showing a drastic decrease in α-helices and increase in β-sheets and random coils. Above 80 °C, the

dx.doi.org/10.1021/jp304339t | J. Phys. Chem. B 2012, 116, 12381–12388

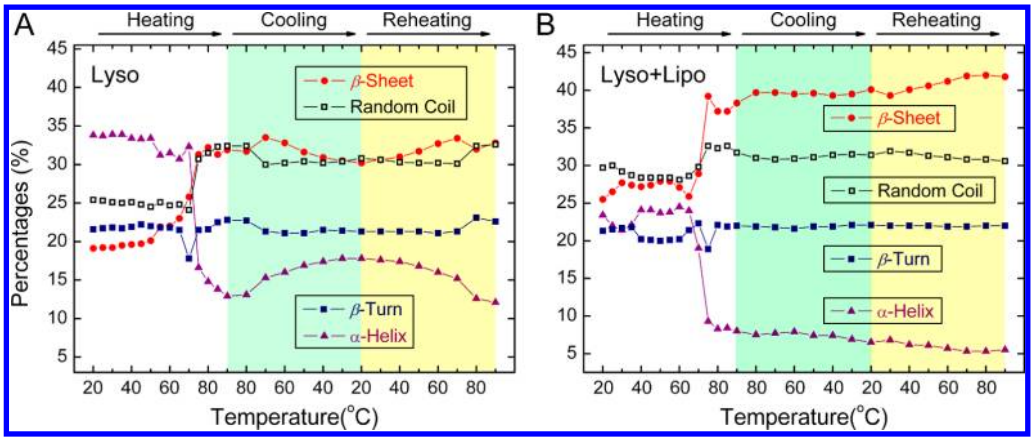

Figure 5. Secondary structural changes of (A) the free lysozyme (ex situ) and (B) the liposome-bound lysozyme (in situ) in heating−cooling−reheating scans measured by far-UV CD.

unfolded structures of the liposome-bound lysozyme pose notable contrasts to those of the free lysozyme: the former has more β-sheets (~40%) than the latter (~32%), but has ~10% less α-helices. The increase in β-sheets and the decrease in α-helices observed in both the native and unfolded liposome-bound lysozymes are undoubtedly associated with membrane binding. The protein molecules tend to unfold/fold into a structure/conformation that maximizes their contact and binding with the membrane surface. β-Sheet is a flat structure with residues on both sides of the plane, which can increase the protein−membrane binding surface, and is thus most favored in the protein−membrane interaction.

Moreover, the free lysozyme shows partially reversible transitions between α-helices and β-sheets in the cooling and reheating scans. In the cooling scan, α-helices gradually increased by ~5%, and meanwhile, β-sheets, random coils, and β-turns all show a slight decrease. This trend is reversed in the reheating scan. But the secondary structures of the unfolded liposome-bound lysozyme are much more "rigid" in the cooling and reheating scans, as no reversible changes are observed. After binding to liposomes, the unfolded proteins are fastened by membranes via electrostatic binding, and thus any fluctuation of the secondary structures is hindered.

Near-UV CD spectra, characterizing the microenvironmental conditions around the aromatic amino acid residues, reflect qualitatively the tertiary structures of proteins. As shown in Figure 6, the tertiary structures of lysozyme are also affected by liposome binding. We can see that the native free lysozyme exhibits a strong positive peak at ~290 nm (Figure 6A). This peak disappears and the curve above 260 nm becomes flat at 90 °C, suggesting the loss of the native tertiary structures. When the sample was cooled to 20 °C, a new broad positive profile appears at 280−330 nm, representing the particular tertiary structures which are different from the native tertiary structures. Then in the reheating scan, the loss of tertiary structures seems to be incomplete, indicating that the tertiary structures formed upon cooling are a little stiff to unfold. But after binding to liposomes, distinct changes in tertiary structure of lysozyme can be seen in the heating−cooling−reheating scans (Figure 6B). First, at 20 °C, the peak (at ~290 nm) of the native liposome-bound lysozyme is weaker than that of the native free lysozyme. Second, at 90 °C, the spectrum shows a new broad peak that is totally different from that of the free lysozyme at this temperature, suggesting that some new and different tertiary structures have formed upon heating. Third, these tertiary

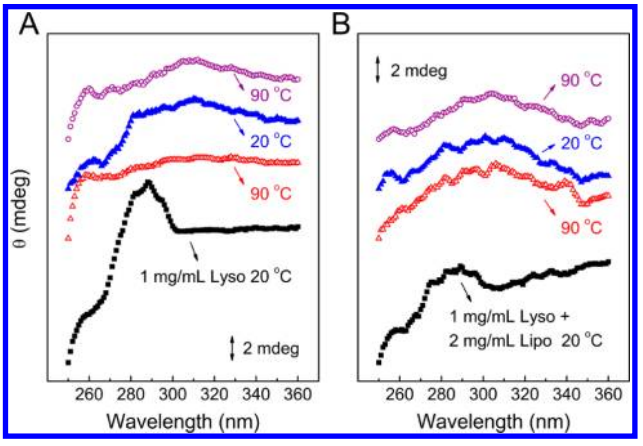

Figure 6. Tertiary structural changes of (A) the free lysozyme (ex situ) and (B) the liposome-bound lysozyme (in situ) in heating−cooling−reheating scans measured by near-UV CD.

structures are very stiff as the profiles of the spectra do not show any change upon cooling and reheating, which is consistent with the far-UV CD results. These results demonstrate that both secondary and tertiary structures of lysozyme are "fastened" by membranes.

3.5. Lysozyme-Induced Lipid Redistribution Requires Particular Thermal History. One interesting feature in Figure 3A is that the enrichment of DPPC was not detected in the first heating scan, but in the cooling and reheating scans. This strongly suggests that a heating process is necessary for lipid redistribution. On one hand, all the lipid molecules change to L_α phase as the temperature rises to above 40 °C, which facilitates the lateral movement (diffusion) of DOPG molecules. On the other hand, at above 65 °C, the structural changes of proteins including unfolding (Figure 5) would affect the lipid phase behaviors. Additional experiments were designed to achieve a better understanding on the lipid phase behaviors of the samples subjected to different thermal treatments.

First, a mixed lysozyme−liposome sample was heated to 55 °C. As shown in Figure 7A, the result of the first heating scan (the black solid line) resembles that in Figure 3A. Then the sample was incubated at this temperature for 1 h, where all the lipids were in the L_α phase with freely lateral movements. After being cooled to 20 °C, the sample was reheated to 55 °C. This procedure allows us to examine the effect of the native

dx.doi.org/10.1021/jp304339t | J. Phys. Chem. B 2012, 116, 12381−12388

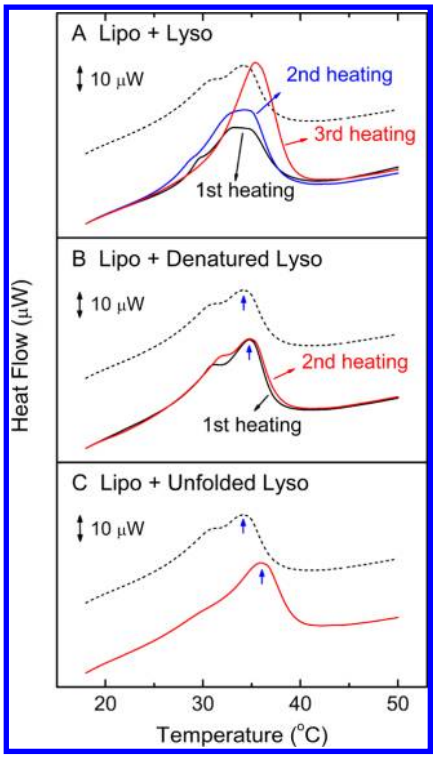

Figure 7. DSC results of the lysozyme–liposome systems with different thermal treatments: (A) the mixed sample was first heated to 55 °C, incubated for 1 h, cooled to 20 °C, and then subjected to the second heating, cooling, and the third heating scans (20–90 °C); (B) lysozyme was heated to 90 °C (ex situ) beforehand and mixed with the liposomes at 20 °C after cooling. The mixed sample underwent a heating–cooling–reheating cycle; (C) lysozyme and liposomes were heated separately to 90 °C (ex situ), and mixed immediately at 90 °C. After cooling, the mixed sample underwent a heating scan. The dash lines are the DSC curve of the free liposomes for comparison.

lysozyme molecules on the thermal behavior of liposomes, since lysozyme remains in native state at 55 °C and lower temperatures (Figure 5). Interestingly, the peak in the second heating scan (the blue line) does not show a significant change in transition temperature except the increase in peak area, which may be due to the increased lipid packing order upon the binding of lysozyme to DOPG. This suggests that the native protein has no capacity to induce lipid redistribution in liposomes. The sample was then further heated to >90 °C to denature the protein, followed by recooling and the third heating scans. Very interestingly, as shown in Figure 7A (the red line), a nice sharper DSC peak is seen in the third heating scan with a remarkably higher peak temperature, exhibiting clearly the phenomenon of lipid redistribution. This means that either the protein unfolded state or the protein unfolding process is necessary for lipid redistribution.

To clarify if the unfolded protein can cause lipid redistribution, a lysozyme solution (2 mg/mL) was heated to above 90 °C and then cooled to room temperature with a scan rate of 1 deg/min, making the protein denature in the absence of liposomes (ex situ denaturation). The predenatured lysozyme was then mixed with liposomes at 20 °C. The DSC curves of this mixed sample are shown in Figure 7B. Compared to the DSC trace of the free liposomes (the dash line), the addition of the predenatured lysozyme does not affect the shape, area, and temperature of the lipid phase transition peak in the first heating scan. A slight change of the peak shape is seen in the second heating scan. It may have resulted from the effect of a tiny amount of the residual native lysozyme on the lipid phase behavior as discussed in section 3.2. This implies that the lipid redistribution is not induced by the ex situ unfolded lysozyme, but rather by the in situ denatured protein. There are two possible mechanisms: (1) the in situ structural changes of membrane-bound lysozyme induce the lipid redistribution; (2) the in situ unfolded state of membrane-bound lysozyme induces the lipid redistribution.

To differentiate these two possible mechanisms, the liposome solution and the lysozyme solution were heated separately to 90 °C at a heating rate of 1 deg/min (ex situ). They were mixed immediately at the temperature where the liposomes were exposed to lysozyme that had just unfolded. Then the mixture was cooled to 20 °C at 1 deg/min. The DSC heating scan of this mixed sample (shown in Figure 7C, the red line) exhibits a thermal profile with a maximum point at 36.0 °C, which is ~3 °C higher than the peak temperature of the DSC profile of the free liposomes (the dash line). But the peak still has a similar shape as that of the free liposomes, which suggests that the enrichment of DOPG under this experimental protocol is not as effective as that in the "in situ" denaturation case. These results reflect that the capacity to induce lipid redistribution is closely linked to a particular thermal treatment or history: an in situ unfolding process is required.

3.6. Mechanism of Protein-Induced Lipid Redistribution. The comparative DSC results in the absence and presence of NaCl (section 3.3) indicate that the lateral redistribution of DOPG is induced via the electrostatic interactions between lysozyme and DOPG. The in situ unfolded lysozyme effectively induces lipid redistribution, but the native lysozyme and the ex situ unfolded lysozyme do not have such ability. These observations strongly suggest that not only the net charge of the protein but also the spatial distribution of charges (the structures of the protein) are important factors.

In the presence of the electric field generated by the DPPC/DOPG membranes, lysozyme unfolds into structures with many more β-sheets and fewer α-helices, and reorganizes into a totally different tertiary structure. The thus obtained unfolded state is more rigid than that of the free lysozyme. It has been found that, in the case of polyelectrolyte, the polymers with a highly charged flat face exhibit highest efficiency in inducing lipid redistribution.[58] In our case of lysozyme, therefore, the structures rich in planar β-sheets formed in the in situ unfolding process should favor the protein–membrane contacts and electrostatic interactions by increasing the contact area. According to previous studies, the positively charged proteins can even form amyloid fibers.[8,35] Although we did not see protein amyloid fibers in the FFEM images, slight protein aggregation might actually have taken place in the lysozyme–liposome interactions, as an increase of ~10% in β-sheet was observed for the membrane-bound lysozyme. The aggregation promoted the formation of intermolecular β-sheets at a larger scale, which should be beneficial to protein–membrane interactions. Besides, more positive residues may be exposed to the surface in contacting with the negatively charged lipids during the in situ unfolding process. All these issues are advantageous to induce the lateral migration of DOPG molecules.

Combining the above results, we have built a schematic model summarizing the mechanism of the lysozyme-induced lipid redistribution (Figure 8): (1) at 20 °C, lysozyme adjusts

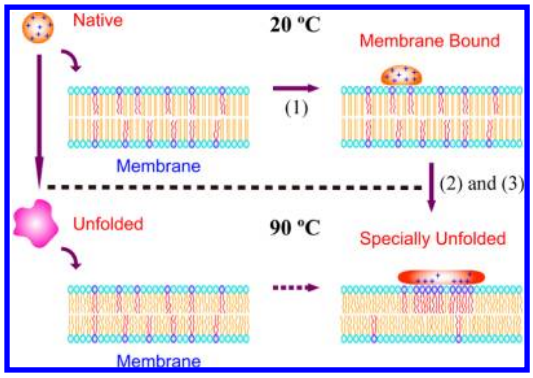

Figure 8. A schematic model depicting the mechanism of the lysozyme-induced lipid redistribution.

its secondary and tertiary structures to achieve a favorable contact/interaction with the lipid membrane; (2) when heated to above 60 °C until 90 °C, the bound lysozyme forms a specially unfolded state with rigid secondary and tertiary structures that are rich in β-sheets, and the positively charged residues may distribute on the face contacting with membranes; (3) this specially unfolded lysozyme induces the flip-flop of DOPG from the inner to the outer leaflet and the lateral redistribution of DOPG in the outer leaflet through strengthened electrostatic attractions. It should be noted that processes 2 and 3 do not proceed separately or stepwise, but simultaneously.

Why is an in situ unfolding process a prerequisite? Why is the membrane-bound lysozyme that has not undergone an unfolding process not able to induce noticeable lipid migration? It is noted that the membrane-induced formation of the specially unfolded structure relies highly on the protein structural flexibility. During the unfolding process, the protein structure has the maximum flexibility. Therefore, in the in situ denaturation case, the final unfolded structure of lysozyme, formed after the most thoroughgoing spatially structural reorganization, is the most advantageous to the protein–membrane contact. The protein structural flexibility decays with the incubation time or the heating–cooling cycle.[52] If the ex situ unfolded lysozyme at 90 °C is immediately mixed with liposomes at that temperature, the unfolded protein structure still retains some flexibility. But the structural reorganization is not as thoroughgoing as in the case of in situ unfolded lysozyme, thus leading to a much weaker extent of DOPG enrichment. This pathway is also added into Figure 8. If the unfolded lysozyme is mixed with liposomes after cooling to 20 °C, protein has lost most structural flexibility. Process 2 is hampered and thus the lipid redistribution cannot be observed (as shown in Figure 7B).

4. CONCLUSIONS AND REMARKS

In this work, we studied in detail the interactions between positively charged lysozyme and a mixed lipid membrane containing the negatively charged DOPG and neutral DPPC. Focus has been mainly on the mechanistic understanding on the protein-induced lipid lateral redistribution. It was found that, unlike the common polyelectrolytes, lysozyme in the static native state has no capacity to induce/enhance the lipid redistribution of DOPG. It is the specially unfolded lysozyme in the presence of negatively charged membranes that is responsible for the lipid redistribution. This specially unfolded lysozyme promotes greatly the protein–membrane electrostatic interaction and lipid lateral migration due to its large contact face and possibly intensively distributed charges on the contact face. The extent of DPPC enrichment is highest in the case of the in situ unfolded lysozyme due to the maximum in the protein structural flexibility in the presence of membrane.

The lipid redistribution or phase separation and other structural changes of biomembranes are widely involved in biological and pathological activities. In this regard, the phenomenon and the underlying mechanism of lipid redistribution induced by specially unfolded protein structures may help to understand the mechanisms of complex bioprocesses such as protein misfolding or amyloid fibrillation. Finally, the understanding gained on lysozyme-induced lipid redistribution may also provide a perspective for studies on the interactions between membranes and other proteins.

AUTHOR INFORMATION

Corresponding Author

*Tel: (+86)10 6279 2492. Fax: (+86)10 6277 1149. E-mail: yuzhw@tsinghua.edu.cn.

Notes

The authors declare no competing financial interest.

ACKNOWLEDGMENTS

We thank Prof. Dong-Sheng Liu and his Ph.D. students for CD measurements and Dr. Shu-Feng Sun for FFEM measurements. This work was supported by grants from the Natural Science Foundation of China (NSFC: 20973100 and 21133009).

REFERENCES

(1) Tamm, L. K. *Protein–Lipid Interactions: From Membrane Domains to Cellular Networks*; WILEY-VCH Verlag GmbH & Co. KGaA: Weinheim, Germany, 2005.
(2) Oellerich, S.; Lecomte, S.; Paternostre, M.; Heimburg, T.; Hildebrandt, P. *J. Phys. Chem. B* **2004**, *108*, 3871–3878.
(3) Charbonneau, D.; Beauregard, M.; Tajmir-Riahi, H. A. *J. Phys. Chem. B* **2009**, *113*, 1777–1784.
(4) Charbonneau, D. M.; Tajmir-Riahi, H. A. *J. Phys. Chem. B* **2010**, *114*, 1148–1155.
(5) Decca, M. B.; Galassi, V. V.; Perduca, M.; Monaco, H. L.; Montich, G. G. *J. Phys. Chem. B* **2010**, *114*, 15141–15150.
(6) Terzi, E.; Hölzemann, G.; Seelig, J. *Biochemistry* **1997**, *36*, 14845–14852.
(7) Seelig, J. *Biochim. Biophys. Acta* **2004**, *1666*, 40–50.
(8) Zhao, H.; Tuominen, E. K. J.; Kinnunen, P. K. J. *Biochemistry* **2004**, *43*, 10302–10307.
(9) Gorbenko, G. P.; Kinnunen, P. K. J. *Chem. Phys. Lipids* **2006**, *141*, 72–82.
(10) Lopes, D. H. J.; Meister, A.; Gohlke, A.; Hauser, A.; Blume, A.; Winter, R. *Biophys. J.* **2007**, *93*, 3132–3141.
(11) Seeger, H. M.; Bortolotti, C. A.; Alessandrini, A.; Facci, P. *J. Phys. Chem. B* **2009**, *113*, 16654–16659.
(12) de Arcuri, B. F.; Vechetti, G. F.; Chehín, R. N.; Goñi, F. M.; Morero, R. D. *Biochem. Biophys. Res. Commun.* **1999**, *262*, 586–590.
(13) Arouri, A.; Kiessling, V.; Tamm, L.; Dathe, M.; Blume, A. *J. Phys. Chem. B* **2011**, *115*, 158–167.
(14) Epand, R. F.; Sarig, H.; Ohana, D.; Papahadjopoulos-Sternberg, B.; Mor, A.; Epand, R. M. *J. Phys. Chem. B* **2011**, *115*, 2287–2293.
(15) Pandey, A. P.; Haque, F.; Rochet, J. C.; Hovis, J. S. *J. Phys. Chem. B* **2011**, *115*, 5886–5893.
(16) Yu, Y.; Vroman, J. A.; Bae, S. C.; Granick, S. *J. Am. Chem. Soc.* **2010**, *132*, 195–201.
(17) Brown, K. L.; Conboy, J. C. *J. Am. Chem. Soc.* **2011**, *133*, 8794–8797.
(18) Yamazaki, V.; Sirenko, O.; Schafer, R. J.; Groves, J. T. *J. Am. Chem. Soc.* **2005**, *127*, 2826–2827.

(19) Forstner, M. B.; Yee, C. K.; Parikh, A. N.; Groves, J. T. *J. Am. Chem. Soc.* **2006**, *128*, 15221−15227.
(20) Yim, H.; Kent, M. S.; Sasaki, D. Y.; Polizzotti, B. D.; Kiick, K. L.; Majewski, J.; Satija, S. *Phys. Rev. Lett.* **2006**, *96*, 198101.
(21) Raudino, A.; Castelli, F. *Colloid Polym. Sci.* **1992**, *270*, 1116−1123.
(22) Polozov, I. V.; Polozova, A. I.; Molotkovsky, J. G.; Epand, R. M. *Biochim. Biophys. Acta* **1997**, *1328*, 125−139.
(23) Epand, R. M.; Rotem, S.; Mor, A.; Berno, B.; Epand, R. F. *J. Am. Chem. Soc.* **2008**, *130*, 14346−14352.
(24) Arouri, A.; Dathe, M.; Blume, A. *Biochim. Biophys. Acta* **2009**, *1788*, 650−659.
(25) Joanne, P.; Galanth, C.; Goasdoué, N.; Nicolas, P.; Sagan, S.; Lavielle, S.; Chassaing, G.; El Amri, C.; Alves, I. D. *Biochim. Biophys. Acta* **2009**, *1788*, 1772−1781.
(26) Haque, F.; Pandey, A. P.; Cambrea, L. R.; Rochet, J. C.; Hovis, J. S. *J. Phys. Chem. B* **2010**, *114*, 4070−4081.
(27) Epand, R. F.; Maloy, W. L.; Ramamoorthy, A.; Epand, R. M. *Biochemistry* **2010**, *49*, 4076−4084.
(28) Oreopoulos, J.; Epand, R. F.; Epand, R. M.; Yip, C. M. *Biophys. J.* **2010**, *98*, 815−823.
(29) Heimburg, T.; Angerstein, B.; Marsh, D. *Biophys. J.* **1999**, *76*, 2575−2586.
(30) Gawrisch, K.; Barry, J. A.; Holte, L. L.; Sinnwell, T.; Bergelson, L. D.; Ferretti, J. A. *Mol. Membr. Biol.* **1995**, *12*, 83−88.
(31) Coutinho, A.; Loura, L. M. S.; Fedorov, A.; Prieto, M. *Biophys. J.* **2008**, *95*, 4726−4736.
(32) Gorbenko, G. P.; Ioffe, V. M.; Molotkovsky, J. G.; Kinnunen, P. K. J. *Biochim. Biophys. Acta* **2008**, *1778*, 1213−1221.
(33) Yaroslavov, A. A.; Sitnikova, T. A.; Rakhnyanskaya, A. A.; Yaroslavova, E. G.; Davydov, D. A.; Burova, T. V.; Grinberg, V. Ya.; Shi, L.; Menger, F. M. *J. Am. Chem. Soc.* **2009**, *131*, 1666−1667.
(34) Gorbenko, G. P.; Ioffe, V. M.; Kinnunen, P. K. J. *Biophys. J.* **2007**, *93*, 140−153.
(35) Zhao, H.; Jutila, A.; Nurminen, T.; Wickström, S. A.; Keski-Oja, J.; Kinnunen, P. K. J. *Biochemistry* **2005**, *44*, 2857−2863.
(36) Alakoskela, J. M.; Jutila, A.; Simonsen, A. C.; Pirneskoski, J.; Pyhäjoki, S.; Turunen, R.; Marttila, S.; Mouritsen, O. G.; Goormaghtigh, E.; Kinnunen, P. K. J. *Biochemistry* **2006**, *45*, 13447−13453.
(37) Litt, J.; Padala, C.; Asuri, P.; Vutukuru, S.; Athmakuri, K.; Kumar, S.; Dordick, J.; Kane, R. S. *J. Am. Chem. Soc.* **2009**, *131*, 7107−7111.
(38) Zhang, X.; Keiderling, T. A. *Biochemistry* **2006**, *45*, 8444−8452.
(39) Ge, N.; Zhang, X.; Keiderling, T. A. *Biochemistry* **2010**, *49*, 8831−8838.
(40) Bergers, J. J.; Vingerhoeds, M. H.; van Bloois, L.; Herron, J. N.; Janssen, L. H. M.; Fischer, M. J. E.; Crommelin, D. J. A. *Biochemistry* **1993**, *32*, 4641−4649.
(41) Hoernke, M.; Schwieger, C.; Kerth, A.; Blume, A. *Biochim. Biophys. Acta* **2012**, *1818*, 1663−1672.
(42) Hasni, I.; Bourassa, P.; Tajmir-Riahi, H. A. *J. Phys. Chem. B* **2011**, *115*, 6683−6690.
(43) Zhang, X.; Ge, N.; Keiderling, T. A. *Biochemistry* **2007**, *46*, 5252−5260.
(44) Kuehner, D. E.; Engmann, J.; Fergg, F.; Wernick, M.; Blanch, H. W.; Prausnitz, J. M. *J. Phys. Chem. B* **1999**, *103*, 1368−1374.
(45) Sharma, U.; Negin, R. S.; Carbeck, J. D. *J. Phys. Chem. B* **2003**, *107*, 4653−4666.
(46) Chaudhary, N.; Nagaraj, R. *Mol. Cell. Biochem.* **2009**, *328*, 209−215.
(47) Yu, Z. W.; Quinn, P. J. *Biophys. J.* **1995**, *69*, 1456−1463.
(48) Fox, C. B.; Uibel, R. H.; Harris, J. M. *J. Phys. Chem. B* **2007**, *111*, 11428−11436.
(49) Findlay, E. J.; Barton, P. G. *Biochemistry* **1978**, *17*, 2400−2405.
(50) Tsonev, L. I.; Tihova, M. G.; Brain, A. P. R.; Yu, Z. W.; Quinn, P. J. *Liq. Cryst.* **1994**, *17*, 717−728.
(51) Wu, R. G.; Chen, L.; Yu, Z. W.; Quinn, P. J. *Biochim. Biophys. Acta* **2006**, *1758*, 764−771.
(52) Luo, J. J.; Wu, F. G.; Yu, J. S.; Wang, R.; Yu, Z. W. *J. Phys. Chem. B* **2011**, *115*, 8901−8909.
(53) Wu, F. G.; Luo, J. J.; Yu, Z. W. *Phys. Chem. Chem. Phys.* **2011**, *13*, 3429−3436.
(54) Sreerama, N.; Venyaminov, S. Y.; Woody, R. W. *Anal. Biochem.* **2000**, *287*, 243−251.
(55) Sreerama, N.; Woody, R. W. *Anal. Biochem.* **2000**, *287*, 252−260.
(56) Sabín, J.; Prieto, G.; Ruso, J. M.; Messina, P. V.; Salgado, F. J.; Nogueira, M.; Costas, M.; Sarmiento, F. *J. Phys. Chem. B* **2009**, *113*, 1655−1661.
(57) Sanderson, P. W.; Lis, L. J.; Quinn, P. J.; Williams, W. P. *Biochim. Biophys. Acta* **1991**, *1067*, 43−50.
(58) Mbamala, E. C.; Ben-Shaul, A.; May, S. *Biophys. J.* **2005**, *88*, 1702−1714.